Journal of Nuclear Medicine, published on December 15, 2022 as doi:10.2967/jnumed.122.264516

Left Ventricular Strain from Myocardial Perfusion Positron Emission Tomography imaging: Method Development and Comparison to 2-Dimensional Echocardiography

1. Jingwen Huang MD[a] , jhuan31@emory.edu
2. Adam J Mitchell MD[b], ajmitc3@emory.edu
3. Ernest V Garcia PhD[c], ernest.garcia@emory.edu
4. C. David Cooke MSEE[c], ccooke@emory.edu
5. Russell Folks BS[c], rfolks@emory.edu
6. Maria Pernetz [d], maria.pernetz@emoryhealthcare.org
7. Abhinav Goyal MD, MHS[b], agoyal4@emory.edu
8. Marina Piccinelli PhD[c], mpiccin@emory.edu
9. Jonathon A Nye PhD[c], jnye@emory.edu

a. Department of Medicine, Emory University School of Medicine, Atlanta, GA
b. Department of Medicine, Division of Cardiology, Emory University School of Medicine, Atlanta, GA
c. Department of Radiology and Imaging Sciences, Emory University School of Medicine, Atlanta, GA
d. Emory Adult Congenital Heart Center, Emory University School of Medicine, Atlanta, GA

Address for Correspondence: Adam J Mitchell MD 1364 Clifton Rd. NE Atlanta, GA 30329 Phone: 404-778-5299 Fax: 404-778-4557 ajmitc3@emory.edu	Contact information for First Author: Jingwen Huang MD 49 Jesse Hill Jr Dr SE Atlanta, GA 30322 Phone: 404-778-5299 Fax: 404-778-4557 jhuan31@emory.edu

Funding: National Heart, Lung, And Blood Institute of the National Institutes of Health under Award Number R01HL143350

Running Title: Strain Analysis from ECG-gated PET MPI

Word count: 4,822

Industry Relationships: Ernest Garcia, C David Cooke and Russell Folks receive royalties from the sale of the Emory Cardiac Toolbox and have equity positions with Syntermed, Inc. The terms of these arrangements have been reviewed and approved by Emory University in accordance with its conflict of interest policies. The remaining authors did not report any conflicts of interest.

ABSTRACT

Objectives: The aim of this study was to develop a measure of longitudinal, radial, and circumferential myocardial strain at rest and during pharmacologic stress using 82Rb-positron emission tomography (PET) electrocardiography-gated myocardial perfusion imaging (MPI). **Methods:** We retrospectively identified 80 patients that underwent rest/regadenoson-stress CT-attenuation corrected 82Rb PET and had a standard resting transthoracic echocardiogram (TTE) with global longitudinal strain analysis within 3 months. A method was developed to compute strain from PET MPI in the longitudinal, radial, and circumferential directions at stress and at rest. PET MPI derived strain and LV function were compared to resting TTE measures as the clinical "reference standard," respectively. Inter-observer agreement of PET MPI strain and left ventricular ejection fraction (LVEF) processing were reported. **Results:** Longitudinal strain assessed with resting TTE GLS showed good correlation with PET MPI at stress (r = 0.68, P < .001) and rest (r = 0.58, P <.001). Resting TTE GLS was also correlated with PET MPI radial strain at stress (r = -0.70, P < .001) and at rest (r = -0.59, P < .001), and with circumferential strain at stress (r = 0.67, P < .001) and at rest (r = 0.69, P < .001). LVEF showed good correlated between resting TTE and PET MPI at stress (r = 0.83, P < .001) and at rest (r = 0.80, P < .001). The Bland-Altman indicated a positive bias of TTE GLS compared to PET MPI longitudinal strain at stress (mean difference = 5.1%, 95%CI = (-2.5,12.7)) and rest (mean difference = 4.2%, 95%CI = (-4.3,12.8)). Reproducibility of PET MPI longitudinal strain showed good agreement at stress (CCC = 0.73, P < .001) and rest (CCC = 0.74, P < .001) with the Bland-Altman showing a small bias in the longitudinal direction at stress (mean difference = -0.2%) and rest (mean difference = -1.0%). **Conclusion:** Strain measured with PET MPI using a novel automated technique correlated well with resting GLS strain obtained by TTE and the measure is reproducible. Strain from PET MPI should be investigated further to establish normal ranges and assess its value in routine clinical practice.

Keywords: Human, Strain, Positron Emission Tomography, Myocardial Perfusion Imaging, Global Longitudinal Strain, Transthoracic Echocardiogram, Rb-82

INTRODUCTION

Left ventricular ejection fraction (LVEF) is a proven measure of global LV function that is associated with long term outcomes. Cardiac diseases affect individuals differently and may not conform to arbitrary EF cutoffs. Therefore, the ability to further categorize a patient's LVEF is needed, particularly in those with EF 35-50% (*1*). Regional LV function parameters such as wall motion and thickening have been shown to contribute incrementally to assessing LV function and categorizing patients' outcomes (*2*). Although powerful, these metrics do not provide one global parameter of LV function that can be easily understood and applied for measuring outcomes.

Echocardiography has an extensive track record in measuring myocardial deformation (i.e., strain). Strain analysis by echocardiography is a functional imaging tool for the clinical assessment of a wide range of cardiac pathologies. Global longitudinal strain (GLS) is most feasibly and robustly measured by speckle-tracking echocardiography and serves as a marker of global function that contributes incrementally to LVEF in the diagnosis and prognosis of cardiac disease (*3*,*4*). GLS has been shown by echo to be a superior predictor of all-cause cardiac mortality compared to LVEF in patients with coronary artery disease (*5*). Additionally, GLS has been shown to be a robust measure for identifying early LV myocardial dysfunction, especially in patients undergoing chemotherapy (*6*).

Myocardial perfusion imaging (MPI), including positron emission tomography (PET) and single photon emission computerized tomography (SPECT), is widely used in assessment of ischemic heart disease, determination of myocardial viability, and evaluation of cardiac device related infections (*7*). Previously, we developed an automated approach to track the LV myocardium throughout the cardiac cycle to measure LV dyssynchrony using electrocardiogram-gated (ECG-gated) MPI (*8*). Here, we expand on this approach using this tracking methodology to measure radial, circumferential, and longitudinal strain at rest and during

pharmacologic stress. We compare PET MPI strain measurements with resting GLS obtained by transthoracic echocardiography (TTE), considered to be the standard of care (*9,10*).

MATERIALS AND METHODS

Patient Population and Study Protocol

In this retrospective study we investigated patients who underwent both TTE GLS analysis and rest/stress 82Rb PET MPI within a 3-month period at our institute between 9/1/2019 and 9/1/2021. Patients who had both studies were excluded if they had major cardiac events (e.g., myocardial infarction, cardiac surgery, revascularization, valve intervention, or starting of chemotherapy) between the time the two studies were completed. This study was approved by the Institutional Review Board of Emory University with a waiver of informed consent based on an assessment of no more than minimal risk.

Strain Measurements

2D Echocardiography and Strain Analysis. Patients were imaged in the left lateral decubitus position with a commercially available echocardiography system (GE Vivid Seven E95, Horten, Norway). Image acquisition was performed using a 3.5 MHz transducer, at a depth of 16 cm in the parasternal view and apical, 2-chamber and 4-chamber views. Standard 2-dimensional (2D), color doppler, and M-mode triggered to the QRS complex, were saved in cine-loop format from three consecutive beats. The LV volumes (end-systolic and end-diastolic) were calculated from the conventional apical 2-chamber and 4-chamber views, and LVEF was calculated with the biplane Simpson's rule (*11*). All measurements were made at rest by research personnel blinded to patient history and outcomes. Resting GLS measurement was performed on apical, two-chamber, four-chamber, and long-axis views using speckle-tracking echocardiography analysis on raw images obtained from patients in real time and were analyzed with commercially available software (GE EchoPAC PC v204), using 2D images at a

frame rate between 55- 65 fps. This software analyzed motion by tracking frame-to-frame movement of natural acoustic markers shown on standard ultrasonic images in two dimensions. Myocardial motion was analyzed using Automated Functional Imaging software within EchoPAC to determine GLS. The LV endocardial border was traced at the end-systolic frame. LV end systolic frame was defined by the left ventricular outflow tract Doppler at the closure of the aortic valve. If necessary, automatic endocardial detection was manually adjusted to assure correct tracking excluding the papillary muscles and chordae and including the LV apex. Longitudinal strain curves were displayed and an experienced echo research personnel evaluated the image quality for satisfactory tracking of the borders.

82Rb PET MPI Study and Strain Analysis. ECG-gated 82Rb PET MPI was performed on a Biograph 40 PET/CT (Siemens Medical Solutions, Knoxville, TN) according to published guidelines (*12*). Patients were instructed to abstain from caffeine or xanthine-containing products for 12 hours as well as beta-blockers and calcium channel blockers for 24 hours. A low dose CT scan was collected prior to the PET study for the purposes of attenuation correction. At rest, approximately 925 to 1,480 MBq of generator produced 82Rb-Chloride was delivered, based on patient weight, intravenously via peripheral radial vein using an automated infusion system (Ruby-Fill, Jubilant Radiopharma, Montreal, Quebec Canada). Hyperemia was induced by intravenous bolus infusion of regadenosine (140ug/kg/min) followed by a second administration of 82Rb-Chloride at the time of peak heart rate. A total of 7-min of data were collected at rest and during hyperemia starting at the time of infusion. Static and ECG-gated images (8 temporal bins) were reconstructed with a non-time-of-flight 2D iterative order-subsets algorithm with attenuation and scatter correction using emission data starting at 2-min post infusion to the end of the data collection.

PET MPI strain measurements were performed using the short-axis LV endocardium detected and tracked throughout the cardiac cycle extracted from ECG-gated PET MPI studies (Figure 1). Automatic detection of the LV endocardium was done using our standard 40 equiangular maximum count circumferential profile detection,

followed by our count-based endocardial border modeling algorithm as used in the Emory Cardiac Toolbox (ECTb) (*8,10,13*). Strain measures were extracted on a point-by-point basis along the radial, circumferential and longitudinal orientations on the rest and stress datasets.

Radial strain analysis uses the maximum counts circumferential profiles extracted from short axis slices. The changes in these counts from each temporal frame along the cardiac cycle have been shown to be linear with myocardial thickening (*14*). The location of these samples is tracked as described above and then translated to their corresponding endocardial position depending on the measured thickening. The thickening for each sample in each frame is added to determine the radial strain at that temporal point. The average radial strain per frame is then calculated as the sum of the strains per frame divided by the number of sample points. Global radial strain is then measured as the temporal maximum of this average strain.

Circumferential strain analysis uses the circumferential samples endocardial locations as in the radial strain above. The spatial distance (L) between each pair of angular samples in each frame is calculated and their maximum separation over the cardiac cycle is assigned as L_o. For each pair of angular samples, strain is then determined using the standard equation Strain = 100% x (L – Lo)/Lo (*15*). The average strain is then determined on a segmental basis for each temporal frame in the cardiac cycle. The average of the sum of the temporal minimum strain for the non-apical segments results in the global circumferential strain. Longitudinal strain analysis starts with the same endocardial samples used for the radial and circumferential strain calculation. These samples are then translated into 40 equiangular long axis planes. Each plane is defined by equidistant endocardial samples from apex to base. The distance between samples is given by the slice thickness, with the total number of samples being given by the length of the LV. This length is different for each angle depending on the distance from base to apex and is also different for each time frame as the LV contracts. This length is interpolated to 20 samples for each base-to-apex length of each of the 40 long axis planes and each of the 8 frames per cardiac cycle. The spatial distance (L) between each pair of interpolated longitudinal samples in each

frame is calculated and their maximum separation over the cardiac cycle is assigned as L_o. The average strain per temporal frame is then calculated by summing the strains over all samples over all longitudinal planes and dividing by the total number of samples. The global longitudinal strain is then determined as the minimum strain over all temporal samples. Note that since both the longitudinal and circumferential strains are negative numbers, their minimum yields the greatest magnitude of the strain measured.

Circumferential and longitudinal strains were calculated in 2D within planes (e.g., within short axis for circumferential strain) for purposes of correlating to 2D measurements by TTE. Radial thickening as measured by the Emory Cardiac Toolbox is inherently a volumetric parameter since it uses count changes throughout the cardiac cycle. These MPI volumetric radial strain measures were correlated to the 2D measures from TTE.

Inter-Observer Reproducibility

All PET MPI strain measures were computed twice by our research team (EG and RF) blinded to the patient condition to examine observer agreement. The Emory Cardiac Toolbox automatically determines processing parameters for the ungated study, and uses these as the starting point for automatic selection of the gated parameters. Each observer had the option to adjust the apex and base slice selection, and left ventricle center and radius for each of the eight gated images. Selection of the base slice location was allowed to change by +/- one slice per gate. Stress and rest parameters, including total slices from based to apex, were matched as best as possible. While all image parameters can affect quantitative results, in strain analysis the most critical appears to be the base selection, and how it is allowed to change during the cardiac cycle.

Statistical Analysis

Continuous variables are reported as mean ± SD or with 95% confidence intervals (95% CI). Bland-Altman analysis, Pearson's correlation, and the concordance correlation coefficient (CCC) were used to evaluate the association and agreement between resting TTE GLS and PET MPI longitudinal, radial, and circumferential

strain and LVEF. CCC and Bland-Altman analysis were used to examine the inter-observer agreement for all three PET MPI strain directions at stress and rest. In the interpretation of the CCC, a value below 0.4 is considered poor; a value between 0.4 to 0.7 is moderate; and a value > 0.7 is good agreement (*16*). For each CCC measure, the 95% confidence interval is reported using the z-transform methods described by Lin et al (*17*). Evaluation of PET MPI strain differences at stress and rest for each direction were determined by examining for non-overlapping confidence intervals which corresponds to a *P*-value < 0.05.

RESULTS

Patient Population

A total of 85 patients were retrospectively identified and 80 patients were included in our study. Three patients were excluded due to a major cardiac event (2 patients had ST-segment elevation myocardial infarction and one patient had coronary artery bypass surgery) between the PET MPI and 2D TTE study. Two patients were excluded as PET MPI and 2D TTE were performed more than 3 months apart. The final population (n=80) consisted of 42 men and 38 women (mean age 62 ± 12). The indications for PET MPI and TTE with strain analysis in these patients include chest pain (50%), preoperative evaluation/ clearance (16%), dyspnea (14%), newly decreased ejection fraction (10%), abnormal ECG findings (4%), palpitations (3%), and syncope (3%). Patient characteristics and summary measures of 2D TTE and PET MPI are given in Table 1.

Strain Measurements

Figures 2, and 3 display the PET MPI strain and TTE processing at rest from a representative patient (80-year-old female with body mass index of 18.1 kg/m^2). In both techniques, strain curves are generated over the cardiac cycle with the PET MPI including the longitudinal, radial, and circumferential directions. Table 2

summarizes the TTE GLS and PET MPI strain measurements. A greater degree of myocardial shortening is reflected by more negative longitudinal and circumferential strain values and more positive radial strain values.

Plots of resting TTE GLS compared to PET MPI strain at stress and rest in the longitudinal direction are shown in Figure 4 with the correlation and agreement summarized in Table 3. The associations of resting TTE GLS with PET MPI were good but showed low agreement at indicated by the CCC. The low agreement can be explained by the presence of a bias between the two longitudinal strain measures, meaning that there is a difference in absolute scale between the modality measures. This bias is more readily observed in the Bland-Alman plots as indicated by the non-zero mean of the measurement differences (figures 4A and 4B). We observed a bias in longitudinal strain between TTE GLS and PET MPI at stress (bias = 5.1%, 95% CI = (-2.5,12.7)) and rest (bias = 4.2%, 95% CI = (-4.3,12.8)) (figures 4C and 4D).

Plots of TTE GLS and PET MPI radial and circumferential strains are shown in Supplemental Figure S1 with the correlations summarized in Supplemental Table 1. There tended to be a higher correlation of resting TTE GLS with PET MPI radial and circumferential strain at stress compared to rest but this was not significant. The negative correlation with radial PET MPI strain is due to comparison of shortening in longitudinal compared to lengthening in the radial directions. No other significant differences were observed between stress and rest PET MPI strain measures.

LVEF measured by resting TTE LVEF showed very good correlation with PET MPI at stress ($r = 0.83$, $P < .001$ and rest ($r = 0.80$, $P < .001$) and good agreement at stress (CCC = 0.71, $P < .001$) and rest (CCC = 0.75, $P < .001$) (figures 5A and 5B). Bland-Altman plots of LVEF from TTE GLS and PET MPI revealed a small bias at stress (mean difference = -8.1%, 95% CI = (-25.6,9.4)) and rest (mean difference = -4.7%, 95% CI = (-22.8,13.5)). (figures 5C and 5D).

Inter-Observer Reproducibility

Inter-observer agreement of PET MPI strain processing from two experienced authors (EG and RF) was good for both stress (CCC = 0.73, 95% CI (0.56,0.91) and rest (CCC = 0.74, 95% CI (0.55,0.93)). The Bland-Altman plots show a minor bias between observers at stress (mean difference = -0.2%, 95% CI (-9.0,8.5)) and rest (mean difference = -1.0%, 95% CI (-8.8,6.8)) indicating good reproducibility of the proposed method (Supplemental Figure S2). Inter-observer agreement of PET MPI strain processing in the radial and circumferential directions were higher than the longitudinal direction but differences were not significant (Supplemental Table 2).

DISCUSSION

In this study, we used PET MPI to compute left ventricular strain in the longitudinal, radial, and circumferential directions at stress and rest. We then compared the strain measured by PET MPI to left ventricular strain measured by 2D TTE. It was demonstrated that PET MPI-based strain measurements strongly correlate with strain obtained by echocardiography. A small bias was observed in the longitudinal strain between the two modalities indicating they were not identical on an absolute scale but this was relatively small compared to the overall strain magnitude. Lastly, the inter-observer reproducibility was lower in the longitudinal direction compared to the radial and circumferential though these differences were not significant. Longitudinal strain is the most difficult of the three directions and is highly dependent on the operator's orientation of the valve plane, which can introduce additional error in the strain calculation reducing the agreement. Other sources of error include differences in how the two datasets are measured, e.g. 2D TTE vs 3D MPI, operator preferences in positioning, particularly, along the valve plane and inherent error in the TTE GLS measure based on published test-retest data (*18*).

An important component of this study is the vendor and software package used to process strain from 2D TTE images. The algorithms used by the different echo manufacturers for measuring strain are considered intellectual property and have never been fully described. Ultrasound methods of measuring strain describe manual length measurements (*19,20*), tissue Doppler (*21*), speckle tracking (*22,23*) or a combination of techniques depending on the vendor package (*24*). This limitation may lead to significant variations between the results from the different manufacturers (*18*). Therefore, we have chosen to develop our PET MPI strain measures from basic principles. Differences in the calculation of strain may, in part, explain the bias observed in the longitudinal strain comparisons but the magnitude of its contribution is unknown. These challenges likely explain our observation of a bias between TTE GLS and PET MPI, which is not unique to our SPECT methods as a bias was also observed when compared to feature tracking with cardiac magnetic resonance (*25*).

Speckle tracking echocardiography has been shown as a useful tool and widely used in clinical studies in measuring heart functions, but some practical limitations to its use exist. First, for 2D strain echocardiography, as cardiac motion is a complicated 3-dimensional (3D) process involving rotation, contraction, and shortening, the direction of the movement occurs not only in the direction of ultrasound beam but also in the direction of the cardiac muscle fiber orientation, creating potential bias. 3D speckle tracking strain echocardiography has been developed but challenges remain such as lower frame rates and lower spatial resolution (*15,26*). Second, a recent study reported a head-to-head comparison of GLS measurements using speckle-tracking echocardiographic software packages from seven different ultrasound machine vendors and showed discrepancies in measuring strain among vendors (*27*). Third, radial and circumferential strain are not typically performed using echocardiography. Circumferential strain use has little incremental information and radial strain are the least reliable and not recommended, with one of the reasons being that the amount of myocardium used for radial strain calculation is significantly less than longitudinal and circumferential (*15*).

In comparison to 2D TTE, PET MPI has the ability to measure global radial, circumferential, and longitudinal strains at both stress and rest and requires no extra information beyond what is collected by standard PET imaging. The use of PET imaging to measure LV strain has not been well-established for routine clinical practice but some publications demonstrated PET study-derived stain in potential clinical settings. Recent publications from Kawakubo and colleagues showed the utility of 13N-ammonia PET MPI to measure LV strain. They studied endocardial strain and used it to compare blood flow and myocardial motility in ischemic patients (*28*). This method is also used to evaluate right ventricular (RV) myocardial longitudinal strain to detect reduced RV myocardial motion due to ischemia in the right coronary artery (RCA) territory (*29*). Separately Kawakubo et al also evaluated the LV strain in heart transplant patients and validated 13N-ammonia PET strains using CMR FT strains (*29*). Compared to previous studies, our study was the first to validate PET MPI-derived strain measurements with resting 2D TTE-derived strain. The addition of strain analysis to the usual PET MPI workflow could be clinically useful to detect subclinical heart failure, evaluate and monitor patients with cardiomyopathy, and further assist characterizing ischemic heart disease.

Several limitations need to be considered in this study. First, we only had 2D strain echocardiography to assess resting GLS and LVEF and correlate with PET strain data. It would be preferred to compare with 3D echocardiographic strain to overcome limitations with 2D TTE. PET studies derived strain can further be compared with cardiac magnetic resonance imaging (CMR) tagging using PET/MR. CMR has been widely accepted as the reference standard imaging modality for strain quantification with the advantage that deformation is directly measured by physical properties of the tissue (*30*). In addition, if the patient's blood pressure is significantly different between PET and TTE studies, this could contribute to differences of strain measurements. PET/CMR can overcome blood pressure issue as the imaging for both studies are processed simultaneously. Second there are technological and physiological differences of how strain studies were acquired, processed, and compared. TTE GLS and PET MPI measurements were obtained at two different time

points up to 3 months apart. Only the resting GLS measurements by TTE were used as the reference standard to compare to stress and rest PET MPI measures of radial, circumferential and longitudinal strain. Although it would be better to have compared all three strain directions individually, resting GLS was the only strain measurement available from the echocardiographic machine used in this study. Nevertheless, resting GLS is the main measurement established to add clinical information beyond LVEF. The rationale for comparing PET MPI measurements of longitudinal, radial, and circumferential strains to TTE measurements of GLS is the mechanical relationship between the three strains expressed mathematically as, (Global Radial Strain + 1) x (Global Circumferential Strain + 1) x (Global Longitudinal Strain + 1) = 1 (*19*). The rationale for comparing PET MPI measures of rest and stress to TTE measures at rest was to determine whether the increased counts in the stress MPI studies over the rest studies improved the correlations with TTE-derived strain and to determine changes in strain between rest and stress.

There are also technical differences between TTE and MPI in how strain is measured due to inherent differences in image formation. TTE has an advantage over MPI for defining the valve plane required for GLS measurements. GLS by TTE is determined from the average of myocardial wall measurements extracted from different planes acquired at different times during the scanning session, whereas MPI global strains are measured from simultaneous acquisition of all LV myocardial walls. MPI has an advantage over TTE in measuring radial strain since MPI uses a count-based method and does not rely on border detection. These technical differences can lead to differences in strain measurements.

Since ECG-gated PET MPI studies were acquired using 8 frames per cardiac cycle, these data are perceived to have low temporal resolution. Our tracking approach, which is common with our previous phase analysis tracking of the dyssynchrony of a specific LV segment, uses continuous Fourier functions to approximate the discrete wall thickening samples. This approach has been shown to have the equivalent temporal resolution of 64 frames per cardiac cycle (*31*). Nevertheless, although our measurement of myocardial strain is mostly count

density dependent, the effect of increasing the number of frames per cardiac cycle to 16 or 32 while maintaining dose and acquisition time constant is yet to be determined. Another perceived limitation is that our count-based analysis cannot be performed in myocardial regions with extremely low tracer concentration due to infarction or severe stress induced hypoperfusion. Our simulations have shown that our tracking approach can separate normal from abnormal thickening in regions with count density as low as 5% of the average normal myocardial uptake (*10*). Although the implication of these findings on the accuracy of strain measurements is yet to be established, the robustness of the tracking used to measure strain is well established.

CONCLUSION

We developed a methodology to measure radial, circumferential and longitudinal strain from ECG-gated 82Rb PET MPI studies. When compared to 2D TTE GLS, longitudinal PET MPI strain had good correlation and was reproducible between observers. There are currently no published reference normal strain values based on 82Rb PET MPI studies and this remains an area of needed development for clinical adoption.

Funding – Research reported in this publication was supported by the National Heart, Lung, And Blood Institute of the National Institutes of Health under Award Number R01HL143350. The content is solely the responsibility of the authors and does not necessarily represent the official views of the National Institutes of Health.

KEYPOINTS

QUESTION: How does longitudinal, radial and circumferential strain measured from ECG-gated 82Rb MPI PET compare to resting 2D TTE GLS?

PERTINENT FINDINGS: Automatic detection of the LV endocardium for the extraction of strain from ECG-gated 82Rb PET MPI was strong associated with resting 2D TTE GLS. A greater degree of myocardial shortening is reflected by more negative longitudinal and circumferential strain values and more positive radial strain values. The interobserver agreement of ECG-gated 82Rb PET MPI strain at rest and stress was very good.

IMPLICATIONS FOR PATIENT CARE: Longitudinal, radial and circumferential strain can be reliably measured from ECG-gated 82Rb MPI PET and may assist with the assessment of global LV function.

Table 1. Baseline characteristics of the patient population.

Demographics	Mean ± SD or n (%)
Age (yrs.)	62 ± 12
Gender (Men %)	42 (52.5)
BSA m^2	2.03 ± 0.3
Days between echocardiography and PET study	14.8 ± 31.7 (range 0-87d)
Diabetes (%)	30 (37.5)
Systolic BP (mm Hg)	132.0 ± 25.4
Diastolic BP (mm Hg)	76.1 ± 12.3
HFrEF (%) - ischemic cardiomyopathy - chemotherapy-induced cardiomyopathy - dilated cardiomyopathy - history of heart transplant	20 (25) - 16 (80) - 2 (10) - 1 (5) - 1 (5)
HFpEF (%)	5 (6.3)
CKD (%)	29 (36.3)
Prior MI (%)	15 (17.5)

Values are mean ± standard deviation (SD) or number (percentage).

Table 2. Baseline measures of left ventricular function from 2D TTE and PET MPI in the patient population.

2D TTE parameters		Mean ± SD
Heart rate		75.8 ± 13.9
LVEF (%)		52 ± 14
LV GLS		-15.0 ± 4.7
End-diastolic LV diameter (cm)		4.8 ± 0.7
End-systolic LV diameter (cm)		3.5 ± 0.9
Interventricular septal thickness-diastolic (cm)		1.2 ± 0.3
LV posterior wall thickness (cm)		1.1 ± 0.3
LV mass index		107 ± 35
82Rb PET ECG-gated MPI parameters		Mean ± SD
Summed Stress Score		5.0 ± 7.2
Summed Rest Score		3.2 ± 4.9
Summed Difference Score		1.8 ± 4.2
Stress	LVEF (%)	60.3 ± 16.1
	Longitudinal strain	-19.7 ± 5.0
	Radial strain	26.6 ± 10.2
	Circumferential strain	-31.5 ± 12.0
Rest	LVEF (%)	57 ± 15
	Longitudinal strain	-18.8 ± 4.9
	Radial strain	21.3 ± 8.0
	Circumferential strain	-28.3 ± 10.3

Values are mean ± standard deviation (SD).

Table 3. Correlation coefficients between resting TTE GLS and strains measured by PET MPI

		Pearson's coefficient	95% CI	*P* value	CCC	95% CI	*P* value
Stress	Longitudinal strain	0.68	(0.54, 0.78)	*P* <.001	0.43	(0.30, 0.57)	*P* <.001
	LVEF (%)	0.83	(0.73, 0.88)	*P* <.001	0.71	(0.52, 0.90)	*P* <.001
Rest	Longitudinal strain	0.58	(0.41, 0.71)	*P* <.001	0.41	(0.27, 0.56)	*P* <.001
	LVEF (%)	0.80	(0.70, 0.87)	*P* <.001	0.75	(0.55, 0.96)	*P* <.001

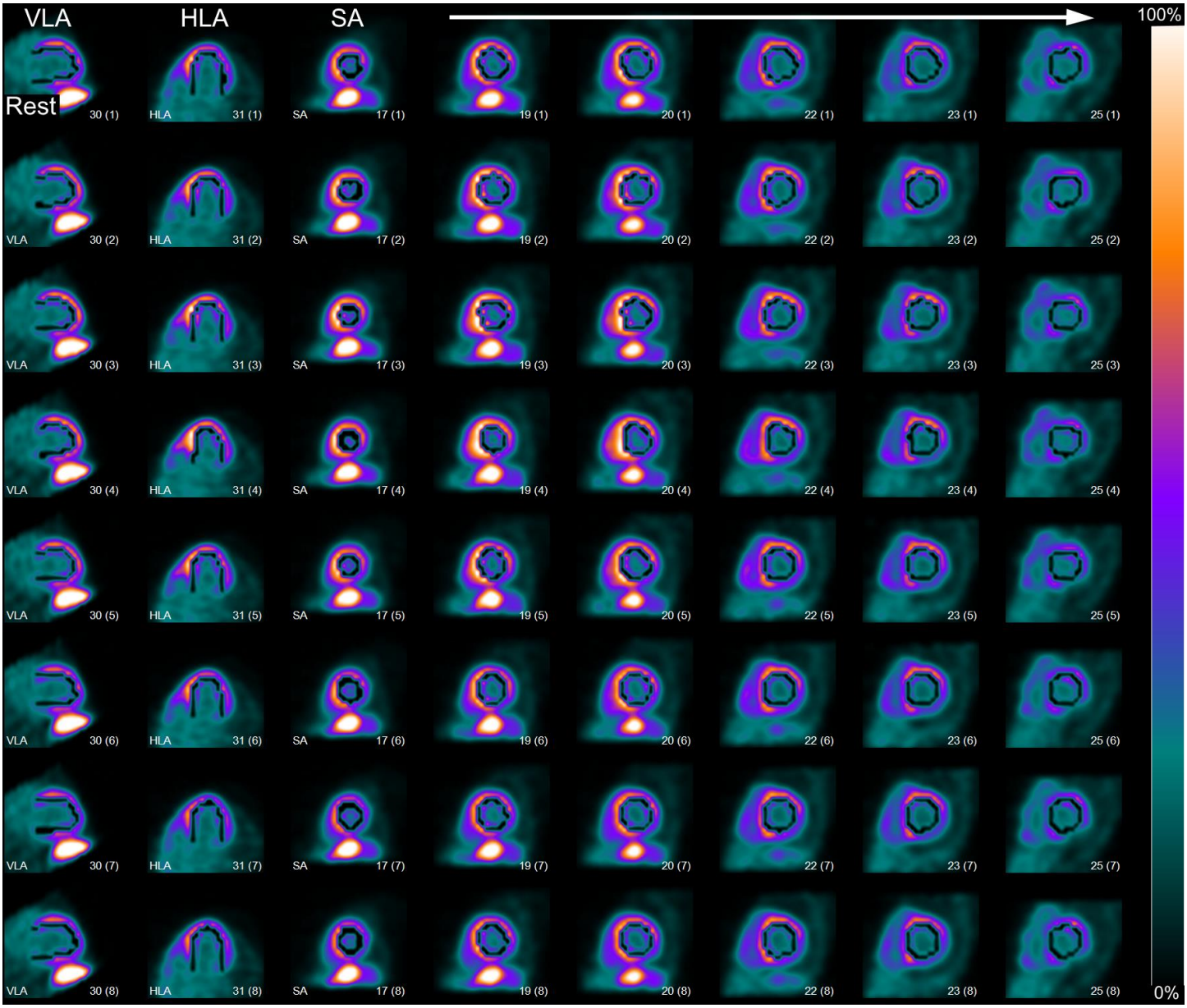

Figure 1. PET MPI strain auto-contours. One patient example demonstrating PET MPI strain contouring methodology. Displayed images are the LV endocardium detection and tracking overlay throughout the cardiac cycle extracted from an ECG-gated PET MPI under rest. Panels show representative vertical (VLA) and horizontal long axis (HLA) slices, followed by short axis (SA) slices from apex to base along the row (white arrow pointing left to right). End-diastolic frames are on the top row followed by contraction to end-systole on middle rows and transitioning back to end-diastole on the bottom row. The colorbar represents min to max normalized counts.

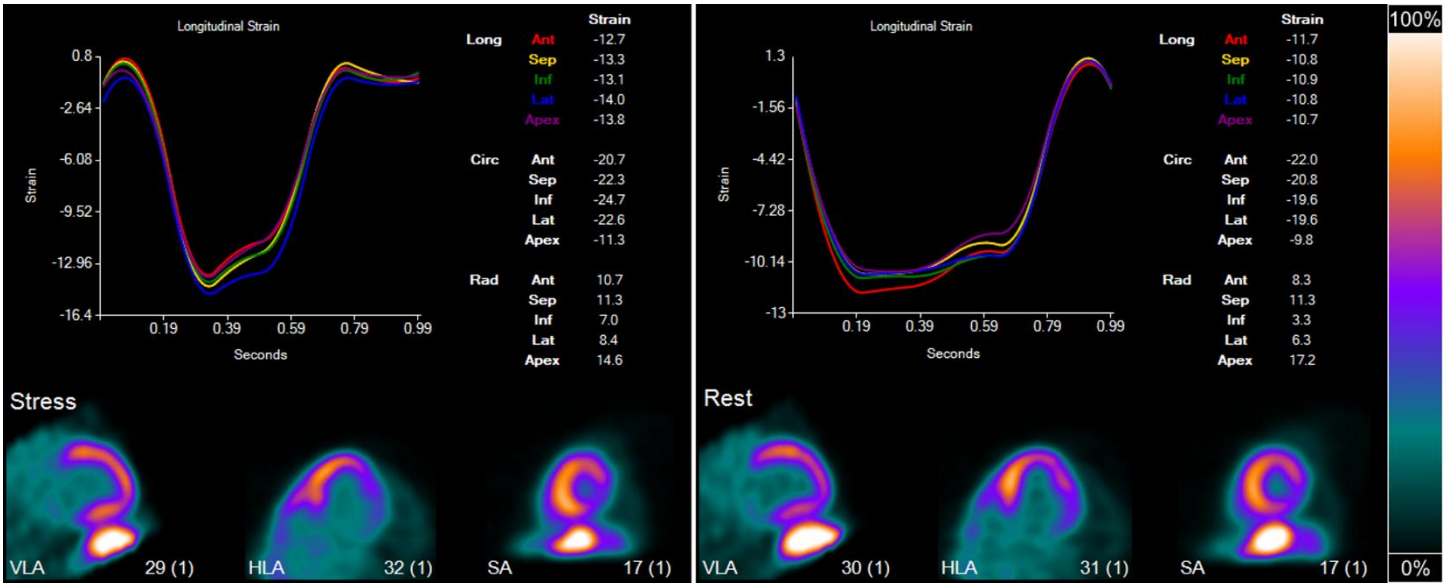

Figure 2. PET MPI Strain. Longitudinal strain curves from the patient example in figure 1 and stress **(A)** and rest (**B**). Length of R-R interval has been normalized to one second. Strain plots over one cardiac cycle are color coded and reported for the anterior (Ant), septal (Sep), inferior (Inf), lateral (Lat), and apical (Apex) regions Circumferential (Circ) and Radial (Rad) strains are also displayed for corresponding myocardial walls but not plotted. The colorbar represents min to max normalized counts.

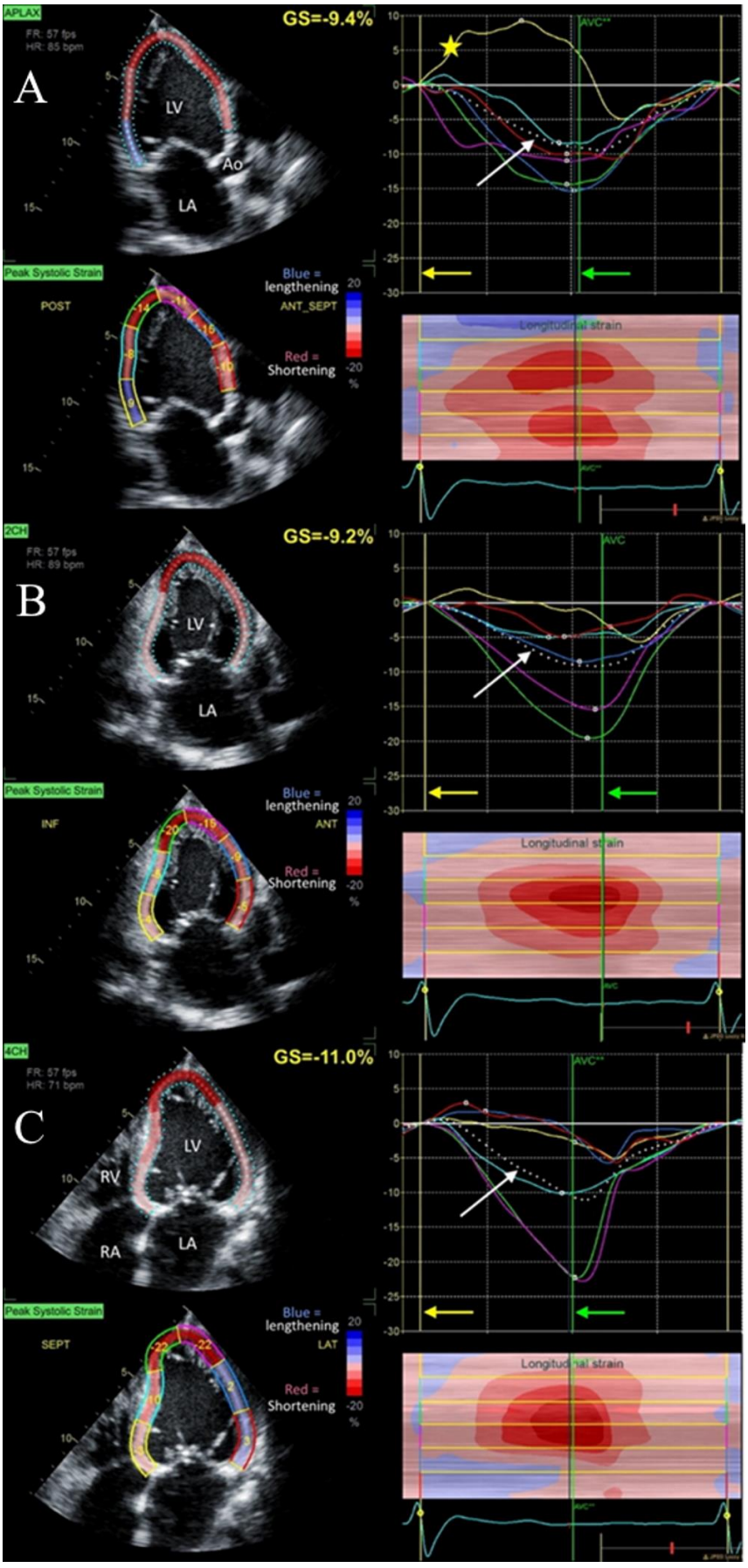
APLAX
FR: 57 fps
HR: 85 bpm
A
LV
Ao
LA
GS=-9.4%
AVC
Peak Systolic Strain
POST
Blue = lengthening
ANT_SEPT
Red = Shortening
20
-20
%
Longitudinal strain
2CH
FR: 57 fps
HR: 89 bpm
B
LV
LA
GS=-9.2%
AVC
Peak Systolic Strain
INF
Blue = lengthening
ANT
Red = Shortening
20
-20
%
Longitudinal strain
4CH
FR: 57 fps
HR: 71 bpm
C
LV
RV
RA
LA
GS=-11.0%
AVC
Peak Systolic Strain
SEPT
Blue = lengthening
LAT
Red = Shortening
20
-20
%
Longitudinal strain

Figure 3. Resting TTE GLS. Rest 2D TTE strain measurements from the patient example in figure 1. LVEF at rest was 32% and GLS at rest -9.9%. Three views, (A) apical, (B) 2-chamber, and (C) 4-chamber, are used in speckle tracking echocardiography and the mean percentage longitudinal strain for each view are presented. Shades of red represent negative strain (contraction) while blue denotes positive strain (relaxation). The white dotted line (white arrows) represents average strain among LV segments during a cardiac cycle. The color of each trace line showing strain corresponds to anatomical color segments on the 2-D color image to the left. The green arrows indicate the aortic valve closure (AVC) line, which indicates end-systole; yellow arrow shows ED line, indicates end-diastole. Note that the yellow star pointed out the yellow curve on apical view-there is abnormal systolic lengthening of the yellow segment (basal inferolateral segment). LA: left atrium; LV: left ventricle; Ao: aorta.

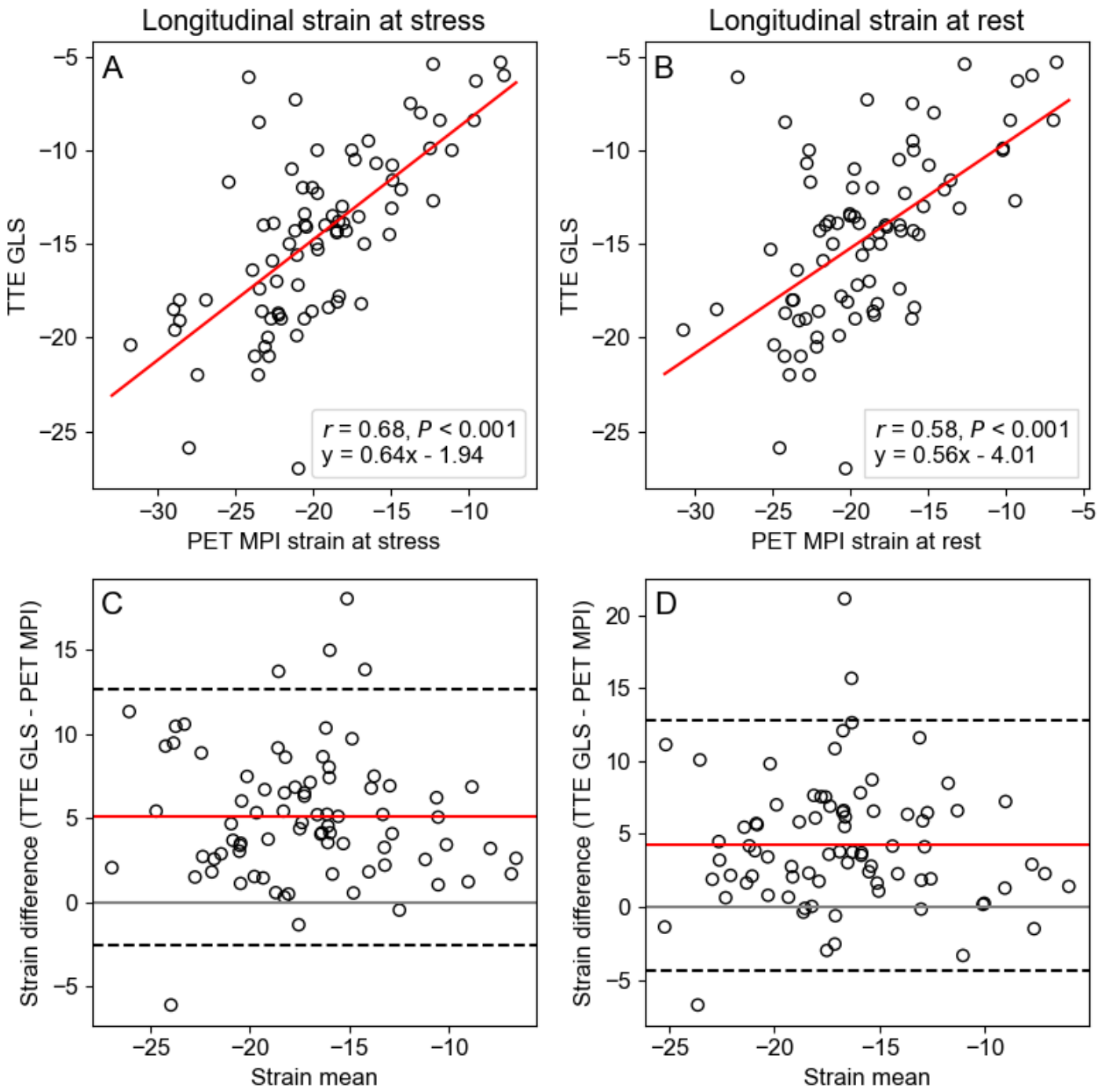

Figure 4. Longitudinal TTE GLS and PET MPI. (A-B) Linear regression plots showing the correlation between longitudinal PET MPI and TTE GLS strain at stress and rest, including the equation of the best fit. (C-D) Bland-Altman plots of longitudinal strain from resting TTE GLS and PET MPI at stress (mean difference = 5.1%, 95%CI = (-2.5,12.7)) and rest (mean difference = 4.2%, 95%CI = (-4.3,12.8)). The red line is the mean

measurement difference and dashed lines are the upper (mean + 2 SD) and lower limits (mean - 2 SD) of the interval of agreement.

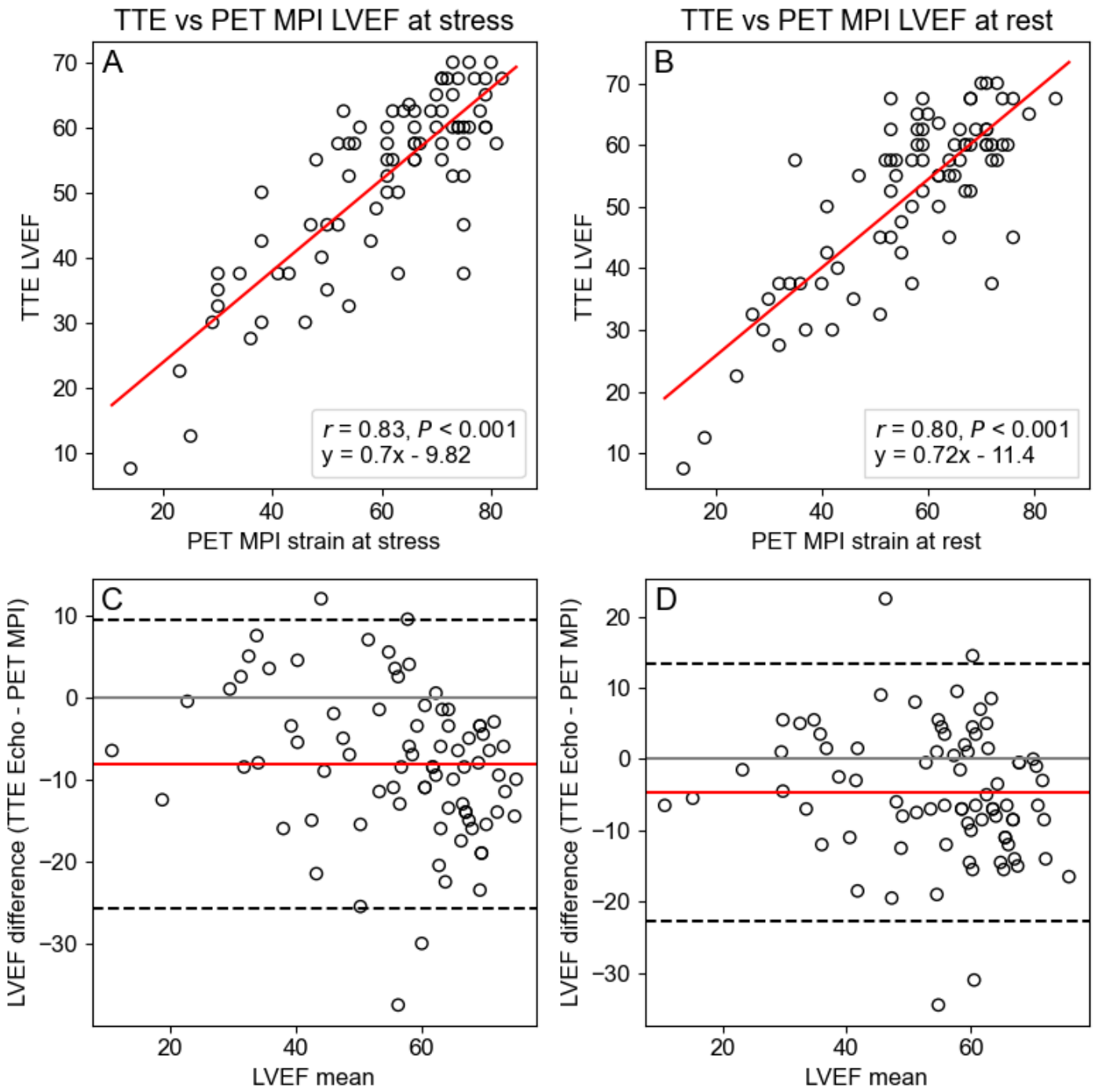

Figure 5. LVEF TTE and PET MPI. (A-B) Linear regression plots showing the correlation between resting TTE and PET MPI LVEF at stress and rest, including the equation of the best fit. (C-D) Bland-Altman plots of LVEF of resting TTE and PET MPI at stress (mean difference = -8.1%, 95% CI = (-25.6,9.4)) and rest (mean

difference = -4.7%, 95% CI = (-22.8,13.5)). The red line is the mean measurement difference and dashed lines are the upper (mean + 2 SD) and lower limits (mean - 2 SD) of the interval of agreement.

References

1. Konstam MA, Abboud FM. Ejection fraction: Misunderstood and overrated (changing the paradigm in categorizing heart failure). *Circulation.* 2017;135:717-719.

2. Cheitlin MD, Armstrong WF, Aurigemma GP, et al. Acc/aha/ase 2003 guideline update for the clinical application of echocardiography: Summary article. A report of the american college of cardiology/american heart association task force on practice guidelines (acc/aha/ase committee to update the 1997 guidelines for the clinical application of echocardiography). *J Am Soc Echocardiogr.* 2003;16:1091-1110.

3. Blessberger H, Binder T. Two dimensional speckle tracking echocardiography: Clinical applications. *Heart.* 2010;96:2032-2040.

4. Zhang KW, French B, May Khan A, et al. Strain improves risk prediction beyond ejection fraction in chronic systolic heart failure. *J Am Heart Assoc.* 2014;3:e000550.

5. Antoni ML, Mollema SA, Delgado V, et al. Prognostic importance of strain and strain rate after acute myocardial infarction. *Eur Heart J.* 2010;31:1640-1647.

6. Sawaya H, Sebag IA, Plana JC, et al. Early detection and prediction of cardiotoxicity in chemotherapy-treated patients. *Am J Cardiol.* 2011;107:1375-1380.

7. Slart R, Glaudemans A, Gheysens O, et al. Procedural recommendations of cardiac pet/ct imaging: Standardization in inflammatory-, infective-, infiltrative-, and innervation- (4is) related cardiovascular diseases: A joint collaboration of the eacvi and the eanm: Summary. *Eur Heart J Cardiovasc Imaging.* 2020;21:1320-1330.

8. Chen J, Garcia EV, Folks RD, et al. Onset of left ventricular mechanical contraction as determined by phase analysis of ecg-gated myocardial perfusion spect imaging: Development of a diagnostic tool for assessment of cardiac mechanical dyssynchrony. *J Nucl Cardiol.* 2005;12:687-695.

9. Santana CA, Folks RD, Garcia EV, et al. Quantitative 82rb pet/ct: Development and validation of myocardial perfusion database. *J Nucl Med.* 2007;48:1122-1128.

10. Cooke CD, Garcia EV, Cullom SJ, Faber TL, Pettigrew RI. Determining the accuracy of calculating systolic wall thickening using a fast fourier transform approximation: A simulation study based on canine and patient data. *J Nucl Med.* 1994;35:1185-1192.

11. Schiller NB, Acquatella H, Ports TA, et al. Left ventricular volume from paired biplane two-dimensional echocardiography. *Circulation.* 1979;60:547-555.

12. Dilsizian V, Bacharach SL, Beanlands RS, et al. Asnc imaging guidelines/snmmi procedure standard for positron emission tomography (pet) nuclear cardiology procedures. *J Nucl Cardiol.* 2016;23:1187-1226.

13. Henneman MM, Chen J, Ypenburg C, et al. Phase analysis of gated myocardial perfusion single-photon emission computed tomography compared with tissue doppler imaging for the assessment of left ventricular dyssynchrony. *J Am Coll Cardiol.* 2007;49:1708-1714.

14. Galt JR, Garcia EV, Robbins WL. Effects of myocardial wall thickness on spect quantification. *IEEE Trans Med Imaging.* 1990;9:144-150.

15. Marwick TH, Kosmala W. 1 - strain imaging applications and techniques. In: Marwick TH, Abraham TP, eds. *Ase's comprehensive strain imaging*. Philadelphia: Elsevier; 2022:1-19.

16. Quinn C, Haber MJ, Pan Y. Use of the concordance correlation coefficient when examining agreement in dyadic research. *Nurs Res.* 2009;58:368-373.

17. Lin LI. A concordance correlation coefficient to evaluate reproducibility. *Biometrics.* 1989;45:255-268.

18. Mirea O, Pagourelias ED, Duchenne J, et al. Variability and reproducibility of segmental longitudinal strain measurement: A report from the eacvi-ase strain standardization task force. *JACC Cardiovasc Imaging.* 2018;11:15-24.

19. Stoylen A, Molmen HE, Dalen H. Left ventricular global strains by linear measurements in three dimensions: Interrelations and relations to age, gender and body size in the hunt study. *Open Heart.* 2019;6:e001050.

20. Aurich M, Fuchs P, Muller-Hennessen M, et al. Unidimensional longitudinal strain: A simple approach for the assessment of longitudinal myocardial deformation by echocardiography. *J Am Soc Echocardiogr.* 2018;31:733-742.

21. Kuznetsova T, Herbots L, Richart T, et al. Left ventricular strain and strain rate in a general population. *Eur Heart J.* 2008;29:2014-2023.

22. Marwick TH, Leano RL, Brown J, et al. Myocardial strain measurement with 2-dimensional speckle-tracking echocardiography: Definition of normal range. *JACC Cardiovasc Imaging.* 2009;2:80-84.

23. Sun JP, Lee AP, Wu C, et al. Quantification of left ventricular regional myocardial function using two-dimensional speckle tracking echocardiography in healthy volunteers--a multi-center study. *Int J Cardiol.* 2013;167:495-501.

24. Dalen H, Thorstensen A, Aase SA, et al. Segmental and global longitudinal strain and strain rate based on echocardiography of 1266 healthy individuals: The hunt study in norway. *Eur J Echocardiogr.* 2010;11:176-183.

25. Onishi T, Saha SK, Delgado-Montero A, et al. Global longitudinal strain and global circumferential strain by speckle-tracking echocardiography and feature-tracking cardiac magnetic resonance imaging: Comparison with left ventricular ejection fraction. *J Am Soc Echocardiogr.* 2015;28:587-596.

26. Saito K, Okura H, Watanabe N, et al. Comprehensive evaluation of left ventricular strain using speckle tracking echocardiography in normal adults: Comparison of three-dimensional and two-dimensional approaches. *J Am Soc Echocardiogr.* 2009;22:1025-1030.

27. Farsalinos KE, Daraban AM, Unlu S, Thomas JD, Badano LP, Voigt JU. Head-to-head comparison of global longitudinal strain measurements among nine different vendors: The eacvi/ase inter-vendor comparison study. *J Am Soc Echocardiogr.* 2015;28:1171-1181, e1172.

28. Kawakubo M, Nagao M, Yamamoto A, et al. (13)n-ammonia positron emission tomography-derived endocardial strain for the assessment of ischemia using feature-tracking in high-resolution cine imaging. *J Nucl Cardiol.* 2021;Epub.

29. Kawakubo M, Nagao M, Kikuchi N, et al. (13)n-ammonia positron emission tomography-derived left-ventricular strain in patients after heart transplantation validated using cardiovascular magnetic resonance feature tracking as reference. *Ann Nucl Med.* 2022;36:70-81.

30. Garot J, Bluemke DA, Osman NF, et al. Fast determination of regional myocardial strain fields from tagged cardiac images using harmonic phase mri. *Circulation.* 2000;101:981-988.

31. Chen J, Faber TL, Cooke CD, Garcia EV. Temporal resolution of multiharmonic phase analysis of ecg-gated myocardial perfusion spect studies. *J Nucl Cardiol.* 2008;15:383-391.

Graphical Abstract